

Role of geophysical methods applied to mapping mineral systems under the Murray Basin cover

R. J. SMITH^{1*} AND K. FRANKCOMBE²

¹Greenfields Geophysics, PO Box 295, Mont Albert, Vic. 3127, Australia.

²Southern Geoscience Consultants, 8 Kearns Crescent, Ardross, WA 6153, Australia.

This paper reviews the role that geophysical methods have played in mapping mineral systems beneath Murray Basin cover in the Stawell corridor of western Victoria. North of Stawell, the Stawell corridor has been shown to extend more than 100 km to the north-northwest, beneath increasing thicknesses of Murray Basin sediments. Based on a geological model developed at Stawell, geophysical methods have played an essential role in mapping new mineral systems in the belt beneath this cover. Regional geophysical data (principally magnetics and gravity) supplied by GeoScience Victoria have been supplemented by company surveys for more detail in selected areas. In addition, various electrical methods have been tested for direct detection of mineralisation beneath deep conductive cover. The results have led to the detection of several mineralised systems many kilometres from outcrop and with no surface expression. Petrophysical measurements on core samples and geophysical logging of drillholes have been essential to the interpretation of geophysical data, and they have also contributed to further understanding of the mineralising processes.

KEY WORDS: electromagnetics, geophysics, gravity, induced polarisation, magnetics, magnetotellurics, petrophysics, Stawell.

INTRODUCTION

The Stawell Goldfield is situated about 245 km north-west of Melbourne in the Delamerian Fold Belt (Miller *et al.* 2006). Most gold production has come from Magdala-type deposits that lie in a corridor that extends both north-northwest and south-southeast from Stawell (Figure 1). Although the geology is well understood around the Magdala mine, outcropping rocks of the Delamerian Fold Belt extend only a short distance north of Stawell before disappearing beneath sediments of the Murray Basin (Swane 2004). These rocks increase in thickness to the north, and exploration in this area relies almost completely on geophysics and drilling.

The geological model developed at Magdala has been used as a basis for further exploration using geophysics and extensive drilling, and this approach has resulted in some significant successes. This paper will discuss the model developed at Magdala and the role geophysical methods have played in exploring similar mineralised systems at Wildwood and Kewell (Figure 1). The geophysical expression of these systems will be illustrated, and some guidelines for ongoing exploration in the area will be developed.

Regional geophysical investigations in the area include deep seismic-reflection profiling as part of the 1997 crustal seismic research program conducted by Geoscience Australia and the Australian Geodynamics

CRC (Korsch *et al.* 2002). The results have been used to develop a structural framework for the Stawell corridor (Murphy *et al.* 2006), but they are not relevant to direct mapping of mineral systems beneath cover and will not be discussed further in this paper.

GEOLOGICAL OUTLINE

Only a brief outline of the geology is included here, as other papers in this thematic issue review the geological evolution of the area in detail (Miller *et al.* 2006). The country rocks surrounding the Stawell goldfield are Cambrian sedimentary rocks that have experienced low-grade metamorphism during the Delamerian and Lachlan Orogenies (Miller *et al.* 2006). These have been intruded by (non-magnetic) granites of Early Devonian age (e.g. the Stawell Granite: Figure 1). They are overlain by flat-lying Tertiary Murray Basin sediments to the north and partly overlain by Tertiary basalts to the south.

Gold mineralisation at Stawell occurs mainly in a highly deformed and altered sedimentary sequence (termed the Stawell Facies) on the western flank of the Magdala basalt dome (Dugdale *et al.* 2006). Sulfides (pyrrhotite) and magnetite in the Stawell Facies contribute to distinctive electrical properties, and the basalt itself has significantly higher magnetic susceptibility and specific gravity than the surrounding sedimentary rocks.

*Corresponding author: greengeo@bigpond.net.au

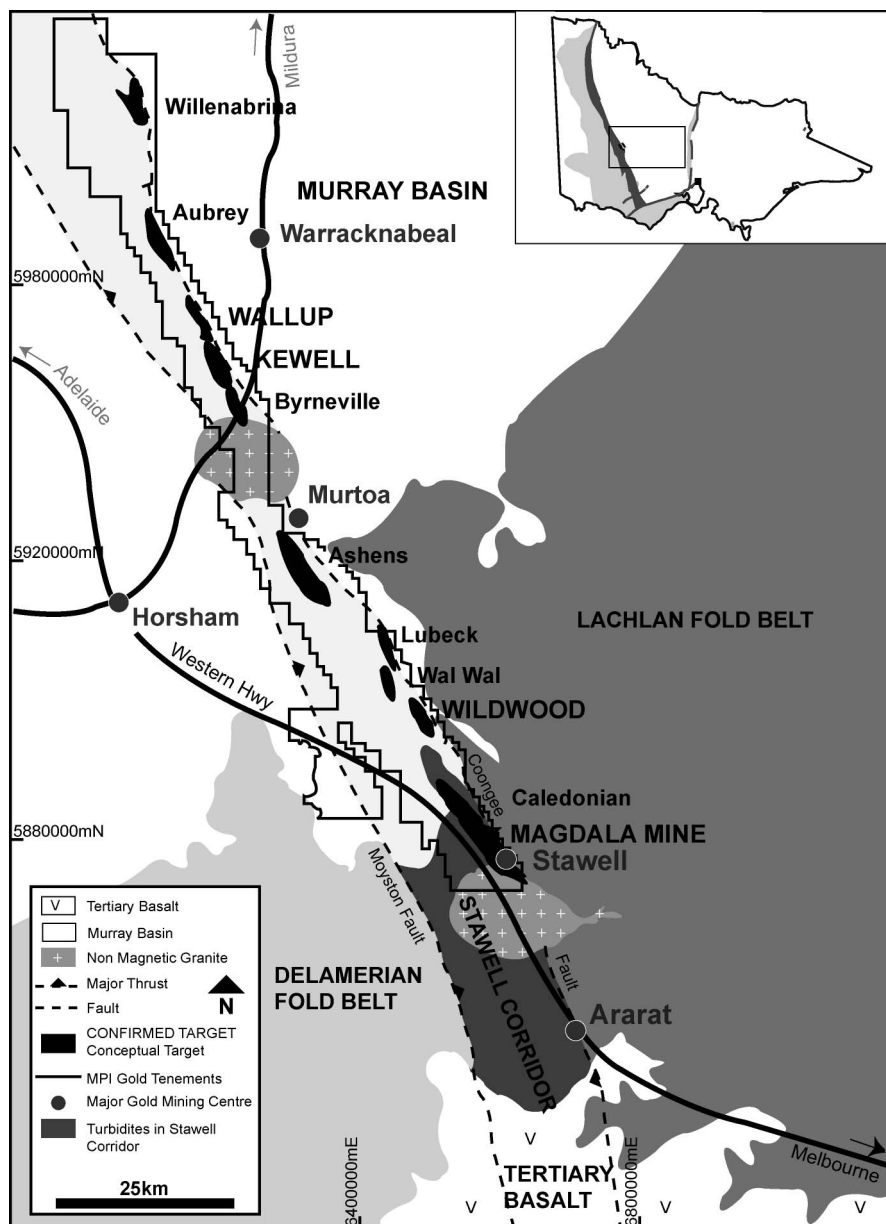


Figure 1 Locality map, Stawell corridor, western Victoria and location of main exploration targets.

Exploration for similar deposits in the area has focused mainly on the location of basalt domes beneath cover, followed by drill testing. This has resulted in several basalt domes being located and investigated, including Wildwood and Kewell (Figure 1). Detailed modelling of the basalt domes has contributed to locating optimal geological environments with potential alteration and associated gold mineralisation. In addition, some geophysical methods have been tested for direct detection of the equivalent of the Stawell Facies beneath cover.

PETROPHYSICS

The earliest reported petrophysical measurements at Stawell were made on seven oriented samples (Robson 1990; Schmidt 1990). The samples were basalt, Stawell Facies and possibly Albion Formation, primarily from Magdala and Wildwood. Most samples showed a high

Königsberger ratio (the ratio of remanent to induced magnetisation), with stable magnetic remanence close to the plane of foliation. Some samples showed reversed magnetisation, but all were approximately in line with the Earth's present field. Although insufficient samples were tested to give totally reliable results, these suggest that the main effect of the remanent magnetisation would be to modify the amplitude rather than change the shape of observed magnetic responses at Magdala and Wildwood.

Additional petrophysical data have been collected at several stages during the current exploration program. This work has included laboratory measurements on samples, downhole logging with a range of tools and also indirect estimation of some physical properties by inversion of geophysical data. Initially, the principal interest was to improve definition of the magnetic properties of the main lithologies, but subsequently the specific gravity, electrical properties and dynamic elastic properties have also been determined.

A suite of 66 core samples from various lithologies (principally at Magdala, Wildwood and Kewell) was selected in August 2002 for the determination of specific gravity, magnetic susceptibility and remanence. Results were reported in Musgrave and Vega (2003a, b), and the mean values are summarised in Table 1.

From the petrophysical data, the main anomalous magnetic and gravity responses are attributed to the basalt and/or Stawell Facies, with a possible contribution from the Albion Formation (Squire & Wilson 2005). They contrast significantly with the Leviathan Formation, which is considered typical of the background response from the more sandy country rocks. Samples of Albion Formation exhibited highly variable magnetic properties, which may correlate with alteration (Dugdale *et al.* 2006) but are not yet well understood. This extreme variability in magnetic properties was also noted in the basalt and Stawell Facies, but they were more widely sampled, and the results are considered reasonably representative.

It is particularly important to note that, as previously observed by Robson (1990) and Schmidt (1990), the magnetic lithologies also have a very high Königsberger ratio (Q) so that the observed magnetic signature is likely to be dominated by remanence. Musgrave and Vega (2003a, p. 2) also noted 'moderate to very high' magnetic susceptibility anisotropy (AMS) in most samples with observed palaeoremanences aligned close to the susceptibility foliation plane. Although the observed magnetic data at Magdala and Wildwood do look relatively normal, observed magnetic responses at Kewell appear more complex and difficult to explain by normal induced magnetisation.

A subset of these samples was also selected for the determination of electrical properties (in addition to specific gravity and magnetic susceptibility). Samples were basalt (with or without visible pyrrhotite), mineralised Stawell Facies, and one sample of mineralised Albion Formation. Results were reported in Emerson (2003) and are summarised in Table 2.

These results were consistent with the values of specific gravity, magnetic susceptibility and Königsberger ratio determined by Musgrave and Vega (2003a, b) (Table 1). A sample of basalt with visible pyrrhotite showed a significant increase in specific gravity, magnetic susceptibility and Königsberger ratio; but this is not considered typical. There was also only

one sample of Albion Formation which, although not statistically significant, gave values consistent with Musgrave and Vega (2003a, b).

The measurements confirmed that the presence of pyrrhotite was closely associated with a significant increase in conductivity and chargeability. When no visible pyrrhotite was present, both the conductivity and chargeability were extremely low and unlikely to be detectable in field measurements. Although it might be anticipated that black shales (possibly graphitic, as they are well recorded in the Ordovician/Silurian metasediments of the Victorian goldfields) could also cause high conductivities and chargeabilities, no samples were available for confirmation.

It was concluded that electrical measurements of conductivity and/or chargeability should be effective in locating pyrrhotite mineralisation (with or without gold) in either Stawell Facies or Albion Formation, provided they could effectively penetrate the overlying conductive Murray Basin sedimentary cover. There may be some other sources of electrical anomalies (e.g. black shale or clays in the weathered zone), but they have not been confirmed to date.

A second suite of 15 samples of basalt and altered sedimentary rocks similar to the Stawell Facies from Wildwood and Kewell was submitted for remanence determination in 2004, and results were summarised in Musgrave (2004). Further analysis of the results from Kewell was undertaken by Grewar (2004). Unfortunately, all samples in this set were affected by a stable remanence component oriented close to the core axis, which is considered to be an artefact. It was probably imposed on the core by exposure to strongly magnetised drill pipe or core barrels, and may not represent the rock properties *in situ*. Further analysis of the results is discussed in Musgrave *et al.* (2006). The origin and orientation of remanence in the magnetic lithologies within the Stawell corridor remains an important problem, and a better understanding is likely to contribute significantly to more detailed magnetic interpretation.

Wireline logging to determine magnetic susceptibility, inductive conductivity, natural gamma and density has been useful at Magdala and several newer prospects, including Wildwood and Kewell (Figure 1). A typical sample log with the complete suite of tools is included in Figure 2. The magnetic susceptibility and conductivity logs exhibit a broad dynamic range. They are presented here with a linear scaling only, which clearly shows the main lithological correlations. More subtle variations can also be perceived with a logarithmic scaling. The results show a clear increase in magnetic susceptibility and density in the basalt and Stawell Facies, and these together are considered to be the main source of magnetic and gravity anomalies. The only significant conductivity anomalies are associated with Stawell Facies or adjacent sedimentary rocks (Albion Formation). Natural-gamma logs are very low in the basalt but generally increase in the alteration zone and the adjacent sedimentary rocks. Detailed examination of the logs has shown some evidence of high gamma activity associated with alteration and mineralisation in and adjacent to faults, but this is not yet well understood.

Table 1 Summarised petrophysical results (from Musgrave & Vega 2003a, b).

Lithology	Density (g/cm ³)	Magnetic susceptibility (SI $\times 10^{-5}$)	Königsberger ratio
Basalt	2.94 ($n = 26$)	718 ($n = 26$)	5.03 ($n = 26$)
Stawell Facies	3.06 ($n = 28$)	2317 ($n = 26$)	9.29 ($n = 26$)
Albion Formation	2.77 ($n = 6$)	322 ($n = 6$)	76 ($n = 6$)
Leviathan Formation	2.76 ($n = 4$)	28 ($n = 4$)	0.21 ($n = 4$)

n , number of samples.

Table 2 Summarised petrophysical results (from Emerson 2003).

Lithology	Density (g/cm ³)	Magnetic susceptibility (SI $\times 10^{-5}$)	Königsberger ratio	Conductivity (S/m)	Chargeability (ms)
Basalt	2.91 (<i>n</i> = 10)	1533.89 (<i>n</i> = 9)	2.67 (<i>n</i> = 10)	0.00 (<i>n</i> = 10)	10.90 (<i>n</i> = 10)
Basalt with pyrrhotite	3.28 (<i>n</i> = 1)	1972.00 (<i>n</i> = 1)	13.30 (<i>n</i> = 1)	400.00 (<i>n</i> = 1)	227.00 (<i>n</i> = 1)
Stawell Facies	3.16 (<i>n</i> = 20)	3228.83 (<i>n</i> = 18)	8.82 (<i>n</i> = 20)	2296.65 (<i>n</i> = 20)	158.40 (<i>n</i> = 20)
Albion Formation	2.82 (<i>n</i> = 1)	132 (<i>n</i> = 1)	30.4 (<i>n</i> = 1)	1 (<i>n</i> = 1)	4 (<i>n</i> = 1)

n, number of samples.

REGIONAL GEOPHYSICS

Regional government geophysical datasets include aeromagnetic and radiometric coverage. The most detailed used 60–80 m terrain clearance and a line spacing of between 200 and 250 m. Although radiometric data were collected with the magnetic data, the Murray Basin cover masks the emissions from the rocks of the Delamerian Fold Belt, and it is therefore of little use when exploring for blind orebodies hosted within them. This regional coverage has been supplemented in the specific areas of interest by detailed company aeromagnetic surveys flown at 35 m terrain clearance on 50 m spaced lines. An image of the resulting data is shown in Figure 3a. The trace of the Moyston Fault is clearly evident to the north of the Stawell Granite as is the dominant response from the Stavely Volcanics to its west. At right angles to the northwest–southeast grain of the Delamerian Fold Belt, strings of Early Devonian diorite intrusions often produce discrete, high-intensity, ovoid magnetic anomalies; some diorite dykes are also known. Many of the narrow ridges running north–south across the grain of the image are strand lines in the Murray Basin cover. The increasing thickness of Murray Basin sediments north of the Stawell Granite causes the character of the image to become smoother to the north, while the high frequency ‘chatter’ to the south of Stawell, around Ararat, is due to Tertiary basalts.

GeoScience Victoria has infilled the Geoscience Australia country-wide 12 km gravity mesh with a 1.5 km network of stations over much of Victoria. This produced an extremely useful dataset from which to target areas for more detailed exploration. The 1.5 km coverage has been further infilled over the selected areas with 50 \times 200 m detailed company surveys. These areas were initially selected by identifying elongate magnetic anomalies with possible associated gravity responses suggesting the presence of basalt domes analogous to Magdala. An image showing a residual gravity dataset created from these combined data is presented in Figure 3b. Again, the Moyston Fault is evident but now can be easily traced to the south of the Stawell Granite. The Coongee Fault is more clearly represented on the gravity image than its magnetic counterpart, as is the relatively low-density Stawell Granite. The northeast–southwest-trending cross-faults that have controlled the emplacement of the Early Devonian diorites are also evident on the gravity image

highlighting their deep-seated nature. At this scale, it is difficult to see the more subtle residual gravity anomalies associated with the specific prospects, but they are shown in more detailed images in Figure 4.

PROSPECT-SCALE GEOPHYSICS

Having used the regional gravity and aeromagnetics to select the prospects, geophysical techniques can then be used to help define drill targets. Three main prospects will be discussed. Magdala is the type area where the exploration model was initially developed and where physical properties were measured on samples and in drillholes. Second, Wildwood is located beneath relatively shallow cover, a few kilometres north of Stawell. Third, Kewell is located 85 km north-northwest of Stawell beneath about 120 m of highly conductive Murray Basin sediments.

Figure 4a shows total magnetic intensity (TMI) and residual gravity images over the Magdala Dome. The Magdala Dome is characterised by both magnetic and residual-gravity high ovoid anomalies. The Stawell Granite to the south is magnetically quiet and has an associated low gravity response. The dendritic patterns in the magnetic image to the northeast and west of the Magdala Dome are the magnetic response from Tertiary palaeochannels containing maghemite and sometimes alluvial gold. A blurring of the magnetic image over the township of Stawell is due to increased terrain clearance required by the civil aviation authorities. The large semicircular anomaly to the southwest of Stawell is caused by a magnetic diorite intrusive which post-dates the weakly magnetic, low-density Stawell Granite. A number of small high-frequency magnetic anomalies on the edge of the Stawell Granite, to the south of Magdala, are due to cultural interference (town rubbish tip, etc.) The quality of the gravity image is degraded by the irregular sampling, although the gravity ridge over the denser basalts at Magdala is still apparent as is the parallel ridge to the east over the Brown’s prospect (Figure 4b).

The mineralised Stawell Facies at Magdala is cut by pyrrhotite veins up to 20 cm thick. Pyrrhotite is an excellent conductor, and this is reflected in the measured conductivity values for the Stawell Facies shown in Table 2 and the wireline log of Figure 2. A trial line of in-loop Transient ElectroMagnetics (TEM) was acquired over the deposit on Line 254 (Figure 4). A conductivity

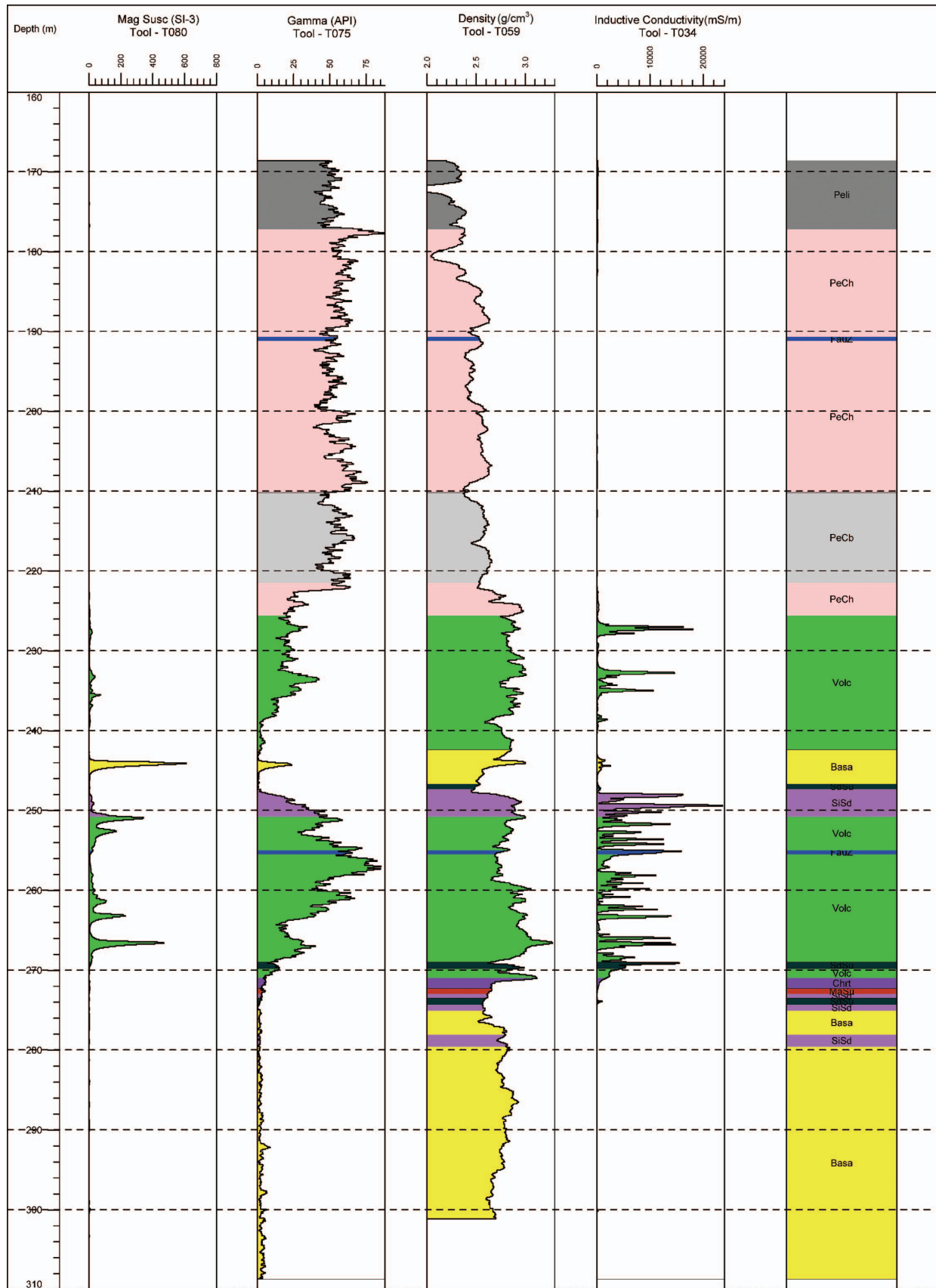


Figure 2 Downhole wireline geophysical logs of drillhole KD038 from Kewell with a simplified geological log. Basalt (Basa) is shown in yellow, 'volcanogenics' with sulfides, equivalent to Stawell Facies (Volc) in green and the remaining Cambrian sedimentary rocks (pelites, Peli, PeCh and PeCb; siliceous rocks, SiSd; sedimentary sulfides, SdSu; chert, Chrt) in pink, grey and mauve. Fault zones are shown in dark blue (FauZ) and massive sulfides (MaSu) in red.

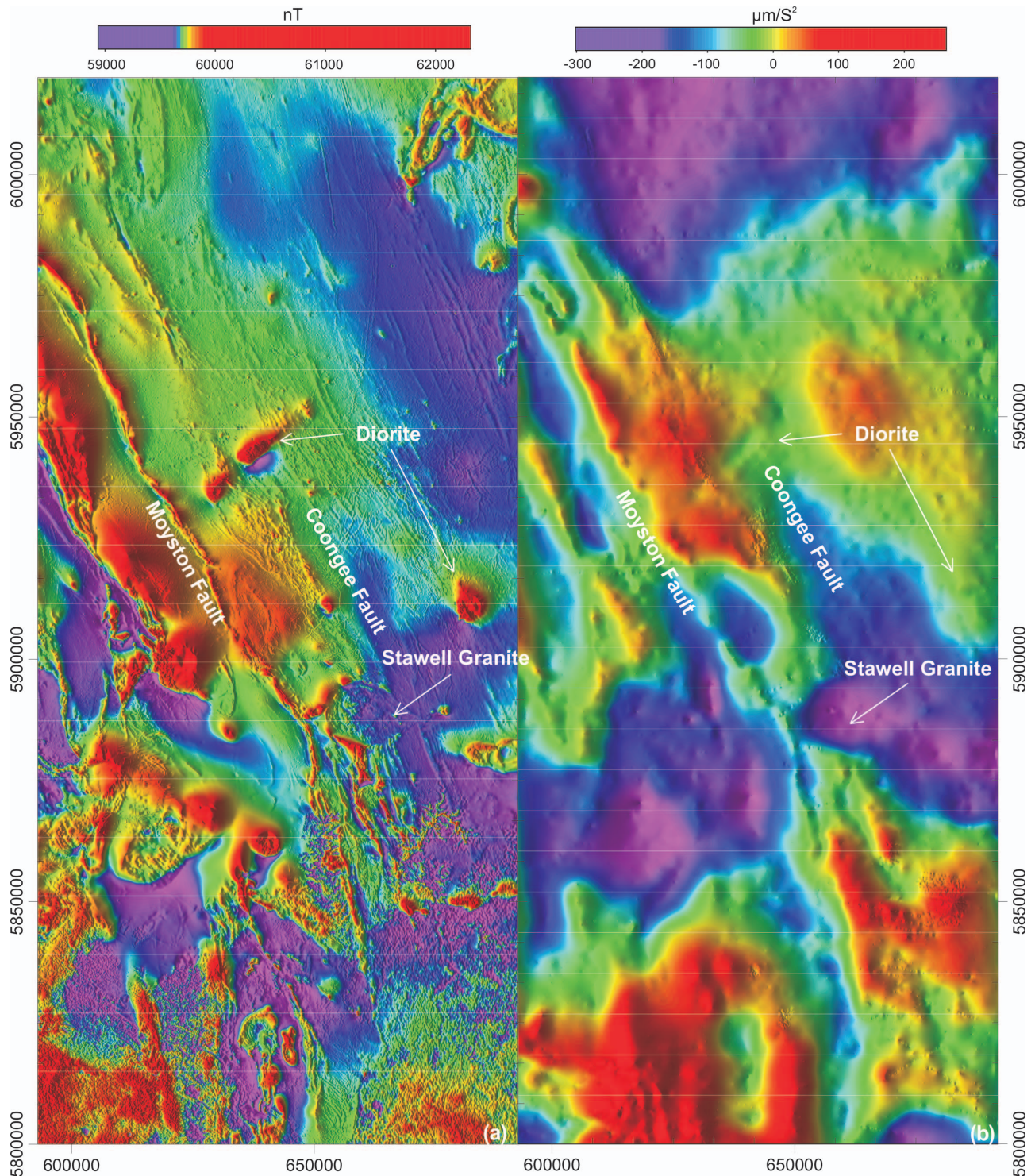


Figure 3 Images of TMI and residual gravity over the Stawell corridor. (a) Image of TMI illuminated from the west. (b) Image of residual Bouguer gravity after removal of a 40 km regional computed at a density of 2.67 t/m^3 . Regional aeromagnetic and gravity data from GeoScience Victoria and Geoscience Australia and detailed surveys provided by Metex and Leviathan Resources.

depth image (CDI) generated from the TEM data is presented in Figure 5a along with a section through a 3D inversion model of the aeromagnetic data (Figure 5b). Gravity coverage over this section is insufficiently detailed, and no gravity inversion model is included. Overlain on both sections are outlines of the basalt

(yellow) and the South Fault (blue) interpreted from drilling and mining. A high-tension power line running to the mine corrupted the TEM data near the crest of Big Hill, causing the data gap in the TEM CDI, at 4900E. The CDI is based on a 1D direct approximation (Nekut 1987) and is not designed to provide an accurate

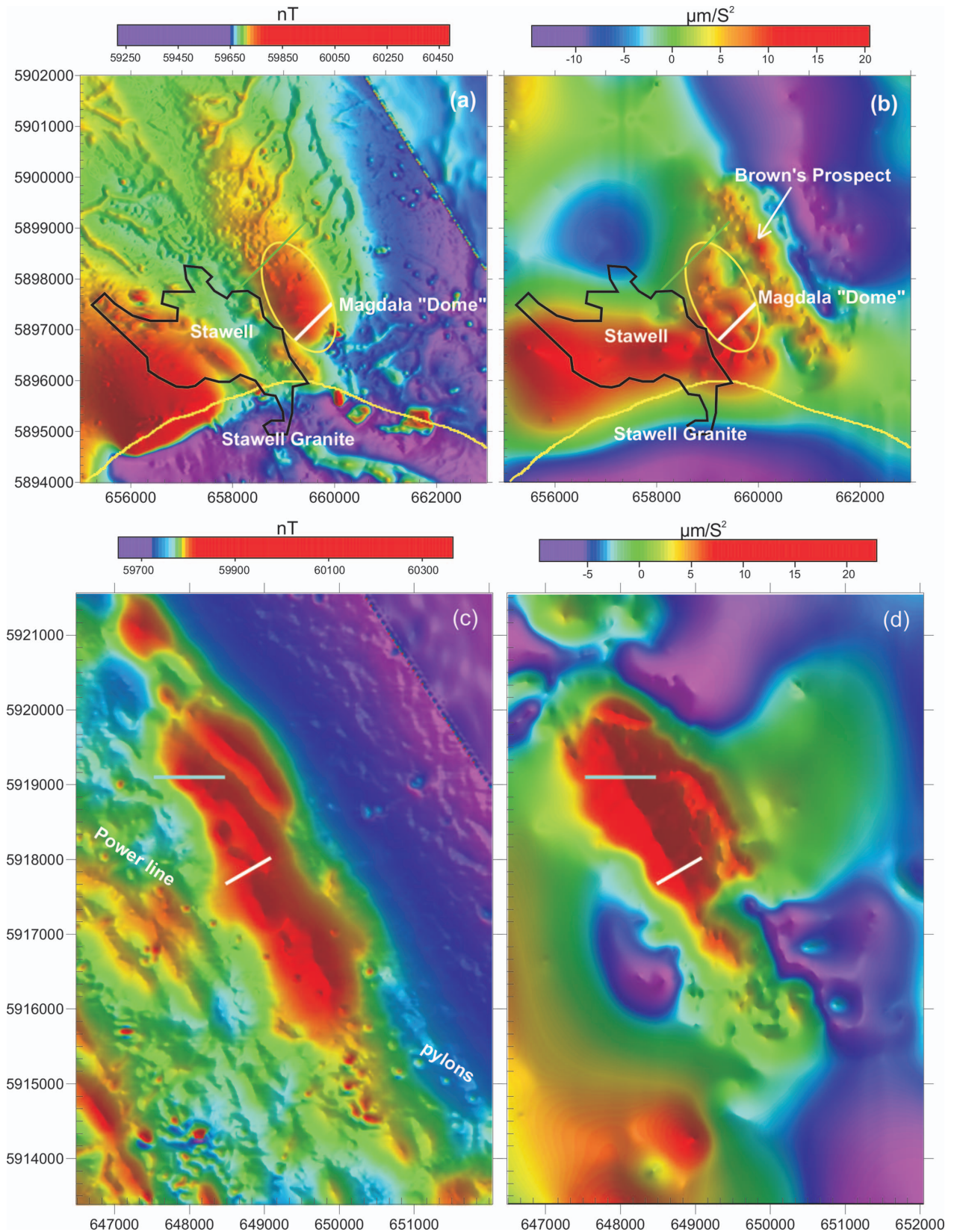


Figure 4 Images of TMI and residual gravity over Magdala and Wildwood. (a) Magdala TMI and (b) Magdala residual gravity illuminated from the east with the location of Line 254 shown in white and Line 320 in green. The town of Stawell is shown as a black outline, and the ovoid magnetic high near the centre of the figure outlines the approximate location of the Magdala dome. (c) Wildwood TMI and (d) Wildwood residual gravity illuminated from the southwest with the location of EM line (white) and IP/AMT (blue). The elongate magnetic high near the centre of the figure coincides with the approximate location of the Wildwood dome.

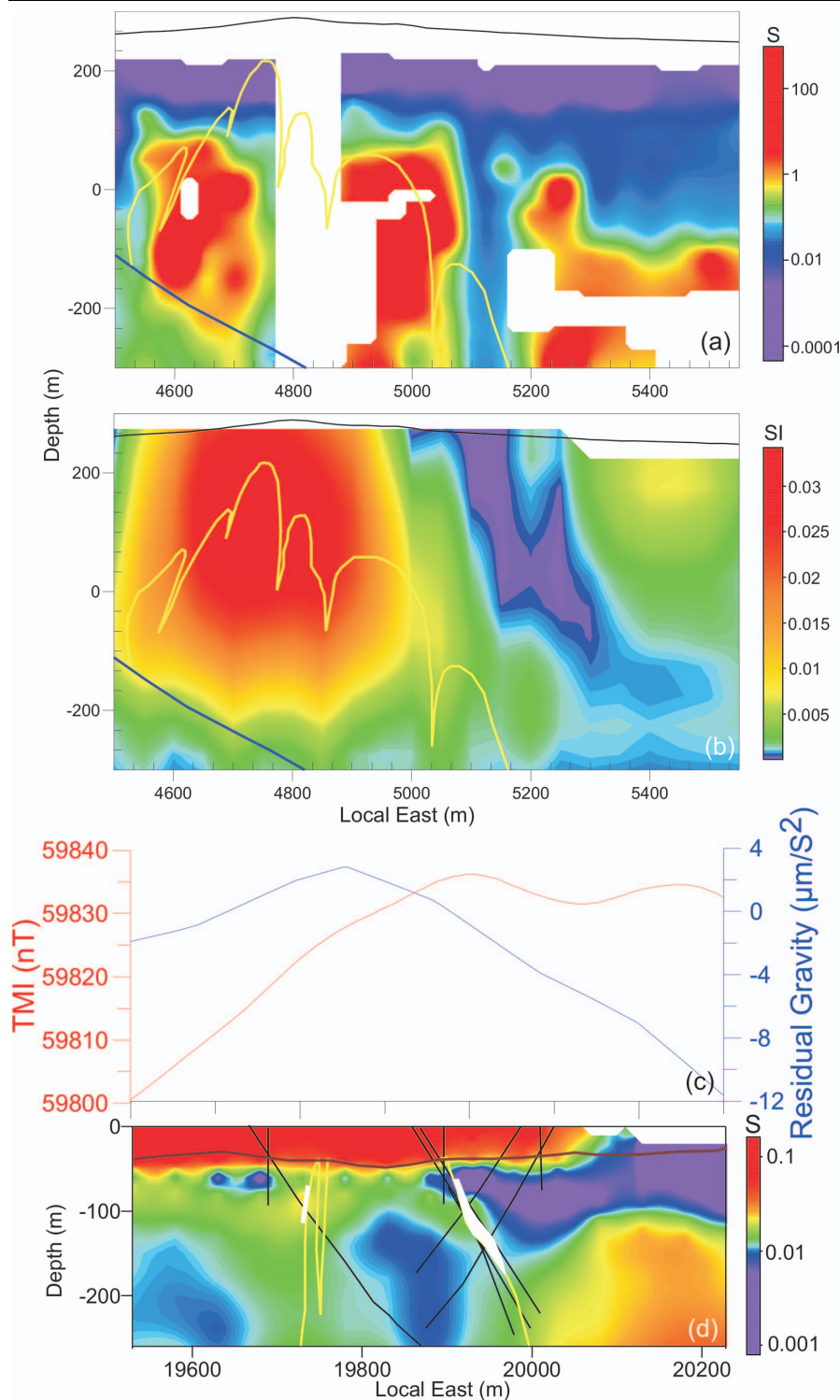


Figure 5 (a) TEM CDI over Magdala Line 254 and (b) vertical section from a 3D magnetic inversion model on Magdala, Line 254. (c) TMI and residual gravity profiles on Wildwood Line 75200 and (d) TEM CDI on Wildwood Line 75200. Warm colours are conductive (a) and (d) or magnetic (b). Interpreted geology is overlain on (a) and (b) with basalt (yellow), South Fault (blue) and ground surface (black). Interpreted geology and drilling are overlain on (d) with basalt outlined in yellow, sulfides (Stawell Facies?) in white and base of transported cover in brown.

representation of the conductivity in a 2D or 3D environment. Nevertheless, it does indicate conductive zones coincident with the thicker parts of the thin layer of Stawell Facies overlying the basalt. The significance of the conductive zone on the eastern side of the CDI is open to interpretation and is yet to be determined by drilling. A clear break evident in both sections at 5100E is interpreted as Albion Formation. Both the magnetic inversion and the CDI have imaged the South Fault remarkably well. This may be simply fortuitous as these

methods do not usually image the base of thick conductors and magnetic units with any precision. This trial line of TEM provided the encouragement to undertake additional surveys on the prospects to the north.

Images of TMI and residual gravity over Wildwood are shown in Figure 5c, d. Small circular magnetic anomalies due to high-tension power-line pylons illustrate the detailed nature of the aeromagnetics. It is immediately clear that the gravity and magnetic

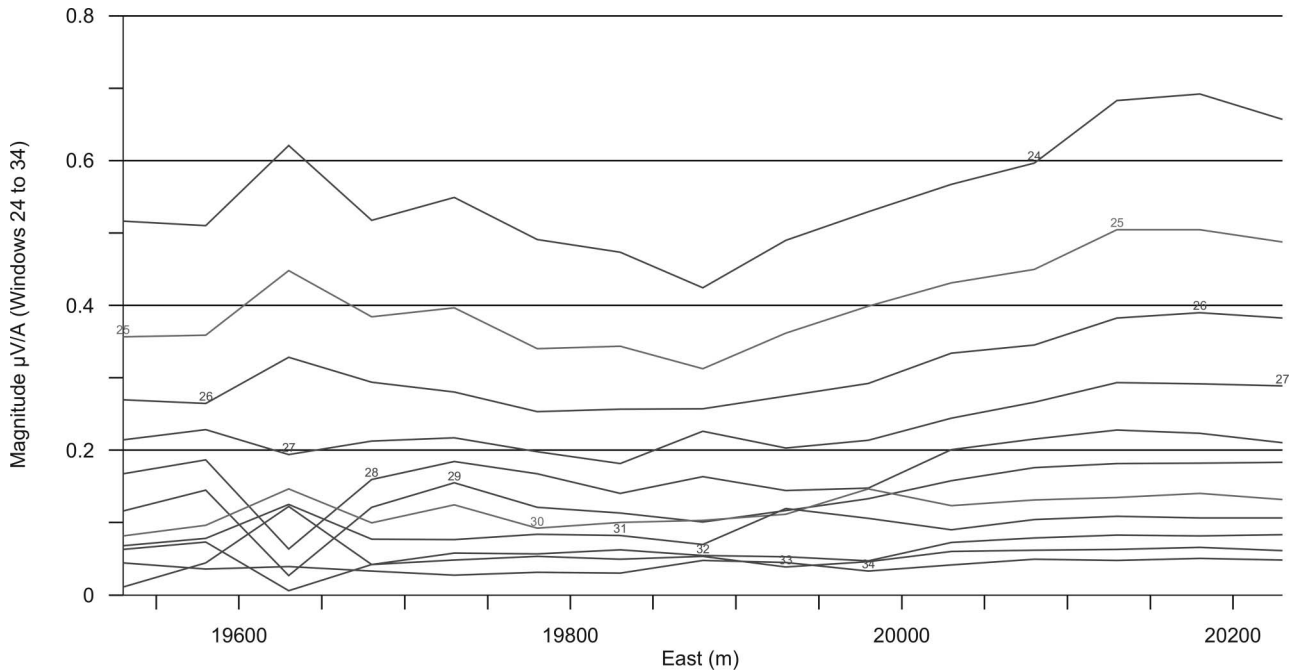


Figure 6 TEM stacked profiles of window amplitude, Line 75200, time windows 24–34, 14.67–126.08 ms.

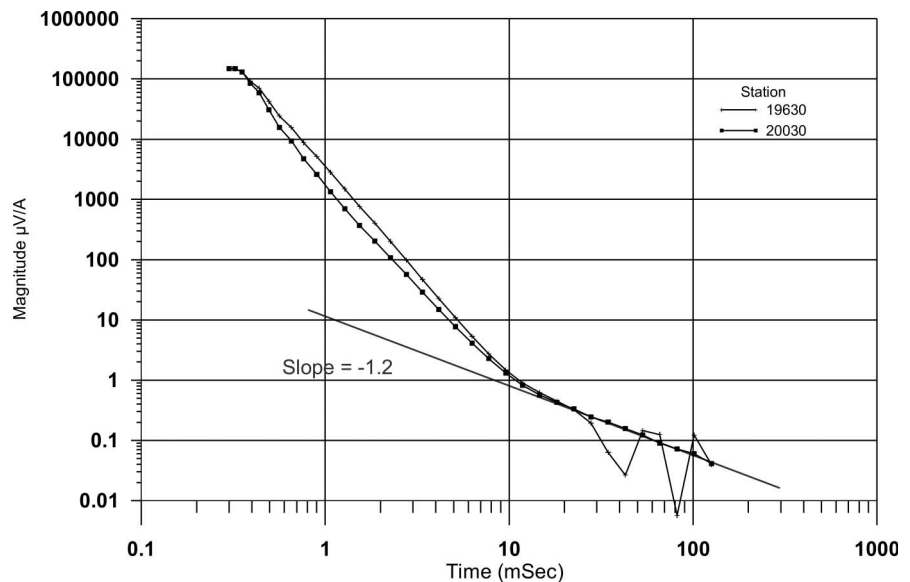


Figure 7 Decay plots for stations 19630 and 20030 from Wildwood line 75200 showing fitted late time power law decay with a slope of -1.2 .

anomalies are different both in overall shape and fine detail. This is interpreted to be due to the presence of magnetic sedimentary rocks (Albion Formation equivalent) which are not as dense as the basalt/alteration package. These sedimentary rocks extend the magnetic anomaly to the south of the gravity anomaly and account for much of the difference between the two datasets.

Following the apparent success of the trial EM line over Magdala, a second trial line was acquired over a weakly mineralised section at Wildwood. Figure 5d shows a CDI created from in-loop TEM data with the current geological interpretation overlain. Also shown (Figure 5c) are profiles of the aeromagnetic response

(red) and residual gravity (blue). Inspection of Figure 4c reveals that the TEM line was close to an interpreted, approximately east–west-trending fault which appears to truncate the basalt and offset the magnetic sediment. This is clearly not the 1D environment assumed by the CDI algorithm; nevertheless, it shows conductive zones that correspond with the shallow sulfide intersections at 19730E and 19920E. It also does an excellent job of mapping the base of the conductive overburden until it becomes too thin to resolve at 20100E. The conductive, magnetic and slightly higher density unit at the eastern end of the section has not been intersected by drilling. It is interpreted to be a sedimentary rock, probably Albion Formation equivalent, as it does not appear to be dense

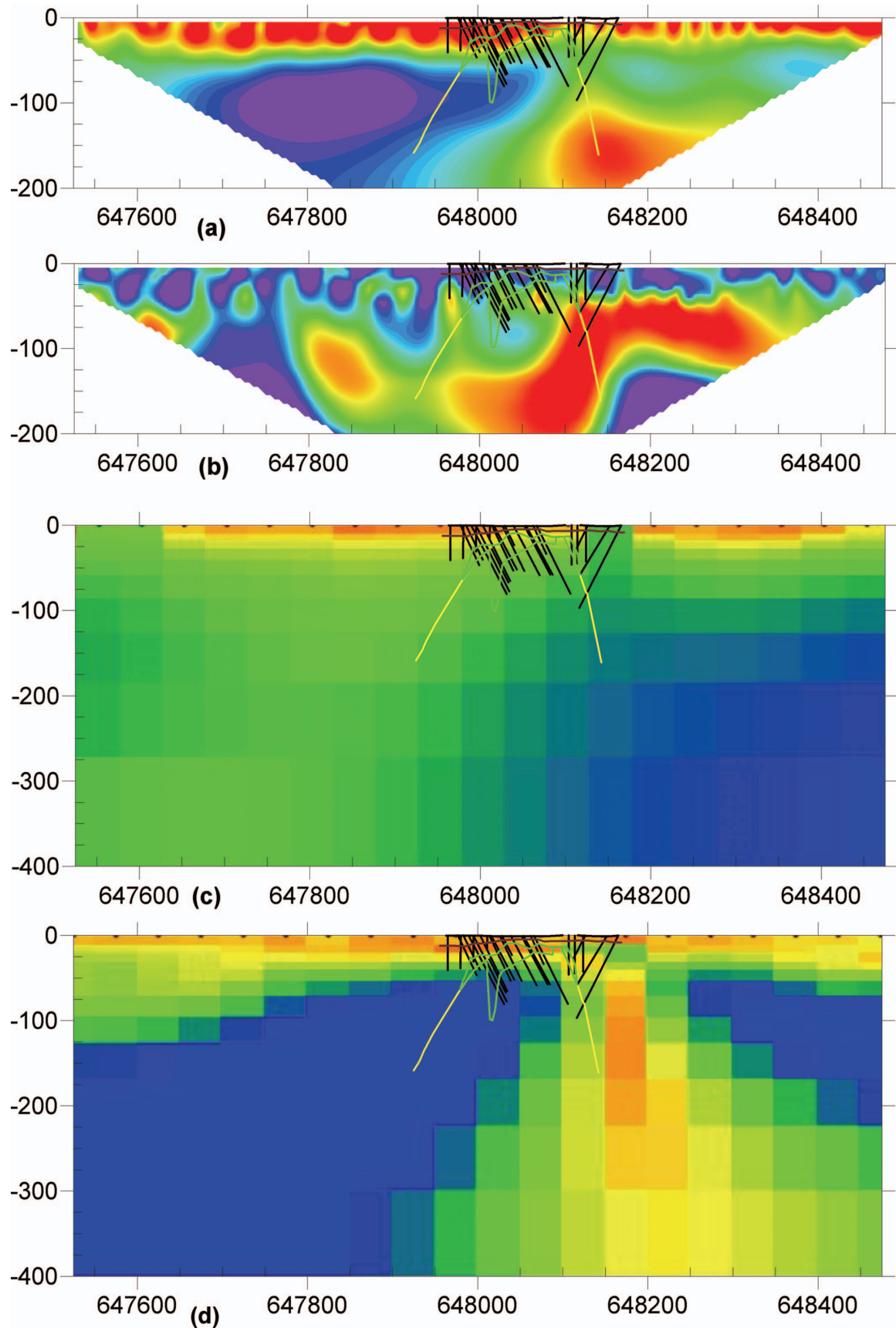


Figure 8 Wildwood line 5919100N, stacked sections from 2D inversion of (a) dipole–dipole resistivity, (b) dipole–dipole chargeability, (c) AMT TE mode and (d) AMT TM mode with geological interpretation overlain. Basalt outlined in yellow, Stawell Facies equivalent in green and base of transported cover in brown. Note dipole–dipole resistivity has warm colours for low resistivity.

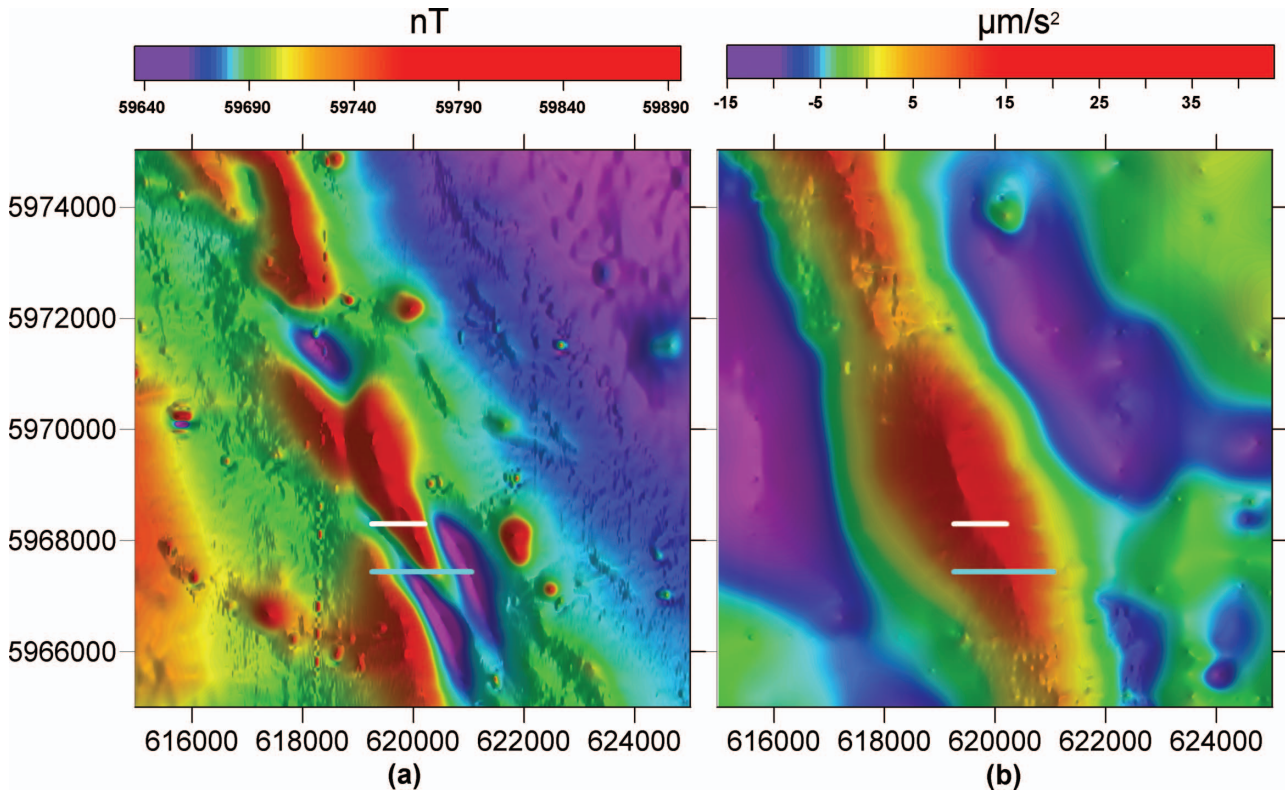


Figure 9 Kewell, images of (a) TMI and (b) residual gravity illuminated from the east. Location of TEM line is shown in white and IP/AMT line in blue.

enough for basalt or Stawell Facies. The apparent conductor at depth beneath 20000E and 20200E can be attributed to a superparamagnetic (SPM) effect from near-surface maghemite (Buselli 1982). TEM profiles for the later time channels (channels 24–34) are shown in Figure 6. The data west of 20000E are noisy, and channels after 26 were not included in the CDI transform. East of 20000E, the profiles are much more regular, and the later channels increase in amplitude, indicating an apparent conductor at depth on the CDI. Figure 7 shows TEM decay curves for station 19630E, a noisy point on the profile, and station 20030E, where the late time decay is more regular. Also shown is a late time, power law fit to the decay for station 20030E, which indicates a decay constant of 1.2; close to the theoretical value of 1 caused by superparamagnetism (SPM), an effect usually ascribed to surficial maghemite. Field inspection at Wildwood confirmed the presence of significant maghemite in the soil, with an increase towards the eastern end of the line. It is rare to observe such SPM effects in central loop TEM data, since they are usually most pronounced close to the transmitter loop. Nevertheless, such a slow rate of decay (t^{-1}) cannot be explained by normal inductive processes, and SPM effects are considered to be the most likely explanation.

Although sulfide mineralisation at Wildwood was not extensive, the depth of cover was also limited, and a trial line of IP and resistivity and audiomagnetotellurics (AMT) was surveyed (location shown in Figure 4c, d). The survey was conducted with dipole–dipole array

(50 m dipoles), using the MIMDAS system (Ritchie 2004). In Figure 8, the top two panels show 2D inversion models for resistivity and chargeability data, respectively. The depth of conductive cover is clearly shown in the resistivity model. Neither of the IP and resistivity models showed a significant response from the known sulfide mineralisation. It is assumed that this is due to the relatively small volume of sulfides present. A deep conductive and chargeable zone is indicated near the eastern contact of the basalt and sediments. The transverse electric (TE) mode AMT model maps the conductive cover quite well but does not detect any conductors at depth. Similarly, the transverse magnetic (TM) mode AMT maps the conductive cover but also indicates a deeper conductor near 648200E, coincident with the conductive and chargeable zone detected by the IP survey. This area has not been extensively drill tested, and the source is not known. It has been suggested that it may be due to weakly disseminated sulfides or graphite in Albion Formation equivalent.

Figure 9 shows images of the TMI and residual gravity over the Kewell Prospect. The main magnetic trend in Figure 9a is a complex combination of positive and negative magnetic anomalies, whereas the gravity image (Figure 9b) shows a single, relatively uncomplicated ridge suggesting a basalt dome. The complex magnetic responses are likely to be caused by remanently magnetised sediments and/or an alteration envelope equivalent to the Stawell Facies. These rocks are foliated and exhibit magnetic anisotropy with

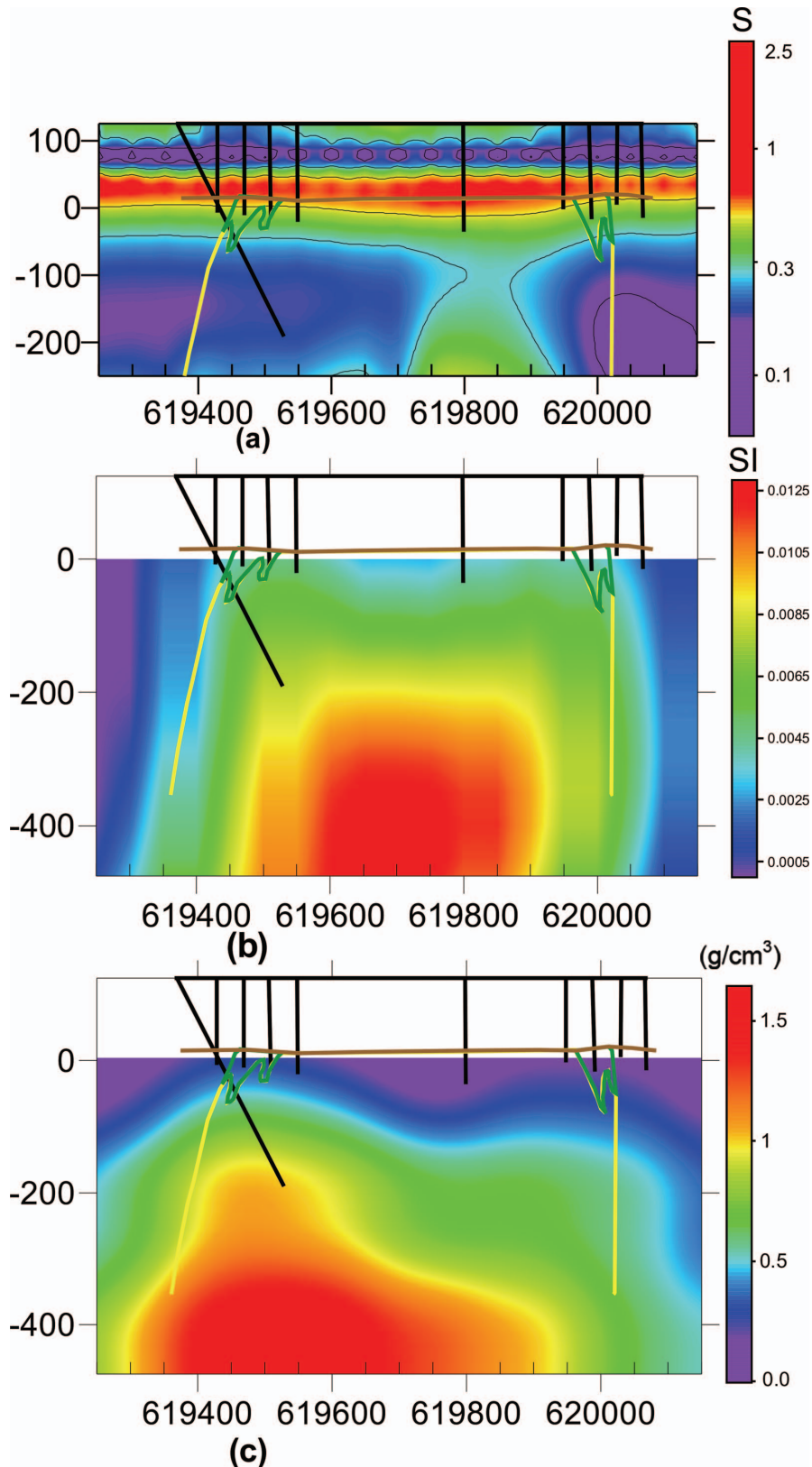


Figure 10 Kewell Line 5968300N sections of (a) TEM CDI, (b) 3D magnetic inversion and (c) 3D gravity inversion overlain by the geological interpretation from drilling. Basalt outline is shown in yellow, Stawell Facies equivalent in green and base of transported cover in brown.

maximum susceptibility close to the plane of foliation. At the southern end of the Kewell dome, the sedimentary rocks and alteration envelope have been shown by drilling to extend continuously across the top of the basalt and its flanks. Further north, the top of the dome has been removed, and only the flanks remain. The

complex magnetic responses at Kewell are not yet fully understood, and work is continuing. Bordering the central magnetic corridor are a number of discrete semicircular anomalies due to Devonian diorite intrusions, as well as high-frequency features coincident with power lines.

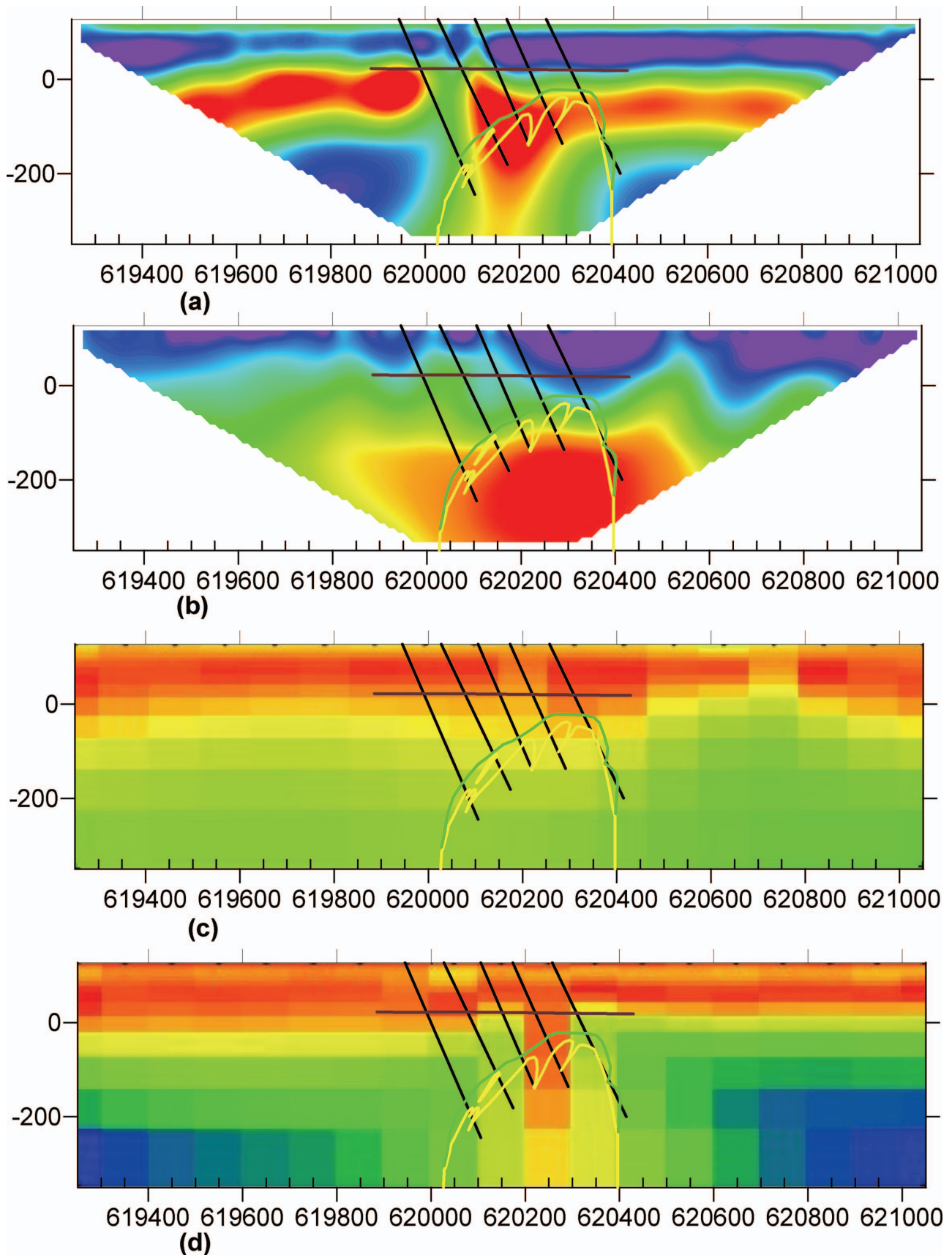


Figure 11 Kewell line 5967440N 2D inversions of (a) dipole-dipole resistivity (hot colours for low resistivity), (b) dipole-dipole chargeability, (c) AMT TE mode and (d) AMT TM mode with geological interpretation and drilling overlain. Basalt outline is shown in yellow, Stawell Facies equivalent in green and base of transported cover in brown.

In-loop TEM data were collected over several lines across the gravity ridge. Figure 10 shows a CDI of one of these lines as well as sections through 3D inversion models of magnetics and gravity over the same line. The TEM has mapped the base of the conductive overburden well and even appears to show Loxton Sands higher in the section, as a near-surface resistor. The source of the weak bedrock conductive zone within the basalt, near 619800E, has not been confirmed by drilling but corresponds with an apparent decrease in density, shown in the gravity inversion. It may be due to fracturing in the basalt or deeper weathering increasing the porosity and thus increasing the relative concentration of saline groundwater in this area. Only minor sulfide mineralisation was known on this line, and the TEM does not appear to have responded to it.

The 3D magnetic and gravity inversion models were constrained to the rocks beneath the Murray Basin sequence; hence the upper levels of the model are blank. Despite remanence dominating the response along strike, at this locality the magnetic inversion outlines the basalt very well.

A trial of IP, resistivity and AMT was conducted on Line 5967440N at Kewell (Figure 11). The method used was similar to measurements at Wildwood, but 100 m dipoles were used in an attempt to penetrate beneath the thicker (~120 m) surficial layer of conductive sediments. The IP and resistivity inversion models both show near-surface horizontal layering due to the Murray Basin sediments, but the thickness is exaggerated. The resistivity model shows a two-layer pattern (resistive overlying conductive) similar to that shown in the CDI (Figure 10a) but with an apparent deeper conductive zone near 620200E. This coincides with an extensive layer of sulfide alteration (equivalent to the Stawell Facies) extending across the top of the basalt dome. The chargeability model also shows a coincident chargeable zone. In this case, chargeability measurements were affected (at high n spacings) by both telluric noise and EM coupling due to the conductive overburden. The IP survey only penetrated effectively over a short central section of the survey line, where valid measurements were achieved to a dipole spacing of >10.

Both TE and TM mode AMT models show a conductive near-surface layer, with the base close to that known from drilling. They also both indicate a deeper conductive zone near 620200E, coincident with the known sulfide mineralisation (only poorly defined in the TE model). No other deep conductors were detected.

CONCLUSIONS

Regional aeromagnetic and gravity data are essential tools in targeting mineralisation beneath the Murray Basin cover. It has been shown to lead directly to the recognition of basalt domes and associated alteration beneath >100 m of cover, at distances of up to 100 km from any outcrop.

At a prospect scale, detailed aeromagnetism and gravity play an important role in lithological mapping. A good understanding of the physical properties of the

target and host lithologies is critical for drill targeting at this stage.

Petrophysical measurements on samples and down-hole wireline logging provide a valuable adjunct to visual geological mapping of core and rock chips as well as providing base values for modelling of the surface geophysical data. More work is required to fully understand the complex magnetic properties of the ore environment and how they may relate to the ore forming processes.

Electrical methods (EM, IP and AMT) can be useful for direct detection of sulfide mineralisation, although their effectiveness decreases as the cover thickens. Tests at Kewell were not conclusive, but they were encouraging. In particular, AMT measurements appeared to be the most effective in penetrating thick conductive cover and detecting the known mineralisation.

Direct detection of alteration haloes beneath thick conductive cover by electrical methods also appears possible, but it remains a challenging task which will receive more attention in the future.

ACKNOWLEDGEMENTS

The support and encouragement of the management of pmd*CRC, Stawell Gold Mines and Leviathan Resources is acknowledged. Without such a visionary management, this exploration program would not have proceeded, and the successes that have been achieved would not have occurred. Permission to publish these results is appreciated.

REFERENCES

- BUSELLI G. 1982. The effect of near surface superparamagnetic material on electromagnetic measurements. *Geophysics* **47**, 1315–1324.
- DUGDALE A. L., WILSON C. J. L. & SQUIRE R. J. 2006. Hydrothermal alteration at the Magdala gold deposit, Stawell, western Victoria. *Australian Journal of Earth Sciences* **53**, 733–757.
- EMERSON D. W. 2003. Report on petrophysical results. Systems Exploration (NSW) Pty Ltd Project 08/2003 (unpubl.).
- GREWAR J. 2004. The stratigraphic, structural, alteration and rock magnetic variations across a basalt-high, Kewell, western Victoria. BSc (Hons) thesis, University of Melbourne, Melbourne (unpubl.).
- KORSCH R. J., BARTON T. J., GRAY D. R., OWEN A. J. & FOSTER D. A. 2002. Geological interpretation of a deep seismic-reflection transect across the boundary between the Delamerian and Lachlan Orogens, in the vicinity of the Grampians, western Victoria. *Australian Journal of the Earth Sciences* **49**, 1057–1075.
- MILLER J. McL., WILSON C. J. L. & DUGDALE L. J. 2006. Stawell gold deposit: a key to unravelling the Cambrian to Early Devonian structural evolution of the western Victorian goldfields. *Australian Journal of Earth Sciences* **53**, 677–695.
- MURPHY F. C., RAWLING T., WILSON C. J. L., DUGDALE L. J. & MILLER J. McL. 2006. 3D structural modelling and implications for targeting gold mineralisation in western Victoria. *Australian Journal of Earth Sciences* **53**, 875–889.
- MUSGRAVE R. J. 2004. Report on remanence analysis of second set of Kewell/Wildwood samples. Report to pmd*CRC, 4 March 2004 (unpubl.).
- MUSGRAVE R. J., GREWAR J. & VEGA M., 2006. Significance of remanence in Stawell goldfield aeromagnetic anomalies. *Australian Journal of Earth Sciences* **53**, 783–797.

- MUSGRAVE R. J. & VEGA M. 2003a. Magnetic petrophysics report; Stawell Project. Report to pmd *CRC, 31 August 2003 (unpubl.).
- MUSGRAVE R. J. & VEGA M. 2003b. Stawell Magnetic Petrophysics Study Remanence Report. Report to pmd *CRC, 1 December 2003 (unpubl.).
- NEKUT A. G. 1987. Direct inversion of time-domain electromagnetic data (short note). *Geophysics* **52**, 1431–1435.
- RITCHIE T. J. 2004. Recent developments in electrical exploration. In: *PACRIM 2004 Proceedings*, pp. 251–256. Australasian Institute of Mining and Metallurgy, Melbourne.
- ROBSON D. F. 1990. Measurement of magnetic remanence from selected rock samples in the Stawell area. Western Mining Corporation Limited, Exploration Division, Minerals (Australasia), Eastern Region, Memorandum **XPR90/40** (unpubl.).
- SCHMIDT P. W. 1990. Magnetic properties of mineralised samples from Stawell. CSIRO Report **PS2-1** (unpubl.).
- SQUIRE R. J. & WILSON C. J. L. 2005. Interaction between collisional orogeneses and convergent margin processes: evolution of the Cambrian proto-Pacific margin of East Gondwana. *Journal of the Geological Society of London* **162**, 749–761.
- SWANE I. P. 2004. Groundwater flow and hydrogeochemistry of the Wimmera Region, Victoria, Australia. PhD thesis, University of Melbourne, Melbourne (unpubl.).

Received 25 August 2005; accepted 26 April 2006